J. Physiol. (1986), **376**, *pp.* 341–357
With 9 text-figures
Printed in Great Britain

INACTIVATION OF THE LOW-THRESHOLD TRANSIENT CALCIUM CURRENT IN RAT SENSORY NEURONES: EVIDENCE FOR A DUAL PROCESS

BY J.-L. BOSSU AND ANNE FELTZ

From the Laboratoire d'Etude des Régulations Physiologiques, associé à l'Université Louis Pasteur, Centre National de la Recherche Scientifique, 23 rue Becquerel, 67087 Strasbourg, France

(*Received 28 February 1985*)

SUMMARY

1. In rat cranial sensory neurones a transient Ca current ($i_{Ca,t}$) is elicited by depolarizing the membrane potential from −80 mV to beyond −50 mV. In this paper the characteristics of the slow and fast inactivation processes of this current are described. Recordings were obtained in whole-cell clamp conditions from Cs-loaded cells. For most experiments, cells were dialysed at an internal pCa of 8, and Na and K currents were eliminated using a choline chloride- and K-free external medium containing 5 mM-Ca and 2 mM-Mg.

2. The decay of $i_{Ca,t}$ could be approximately fitted by a single exponential with a voltage-dependent time constant which decreased from about 150 ms at −50 mV to about 25 ms at −20 mV. This suggests a single process of inactivation but a detailed kinetic analysis of the onset and the offset of the inactivation revealed biphasic processes.

3. The onset of inactivation displays two exponential phases. The fast phase lasts for 100–500 ms, and the slow phase lasts for a few seconds. The relative amplitude and the time constants of each phase vary with the inactivating potential.

4. The recovery from inactivation is also biphasic, with either a fast or a slow component predominating, depending on whether a short- (some hundreds of milliseconds) or a long- (in the order of tens of seconds) inactivating pulse has been used. At −80 mV, after a 300 ms inactivating pulse, responses recover to at least 40% of maximum within 200 ms and recovery is complete within 1 s; after a long pre-depolarization (10–20 s), recovery takes 4–5 s. Fast recovery was observed best after large but brief depolarizations and slow recovery was observed best following long inactivating pre-pulses of small amplitude.

5. The voltage-dependence of slow and fast inactivation was determined by realizing inactivation curves. Fast inactivation developed between −60 and −20 mV while the slow process occurred at more hyperpolarized potentials, e.g. at −75 to −50 mV.

6. Fast inactivation was not altered by the entry of Ca during the previous activation of the channel. Further, decay of $i_{Ca,t}$ was not modified when Ba was substituted for Ca or the internal pCa was decreased. These are indications of a

uniquely voltage-dependent process. A possible role of Ca entry in slow inactivation is discussed.

7. Increasing the internal Ca concentration from 5×10^{-10} to 10^{-7} M differentially shifted both types of inactivation curves towards more hyperpolarized potentials.

8. The two components of inactivation can be identified as two distinct inactivated states of the Ca channel.

INTRODUCTION

Most Ca currents decline with time despite maintained depolarization (see reviews of Hagiwara & Byerly, 1981; Eckert, Tillotson & Brehm, 1981; Tsien, 1983; Eckert & Chad, 1984). In many cases this has been shown to be a result of inactivation of the Ca channels under maintained depolarization. It is a matter of debate as to how this inactivation proceeds. In polychaete eggs, Fox (1981) has shown a voltage-dependent process to be dominant, as it is for the Na channel. Alternatively, inactivation may be mediated through an elevation of the internal Ca concentration (Hagiwara & Nakajima, 1966; Kostyuk & Krishtal, 1977; Takahashi & Yoshii, 1978), possibly as a result of previous entry of Ca (Eckert *et al.* 1981; Ashcroft & Stanfield, 1981; Plant, Standen & Ward, 1983). Evidence for both mechanisms has been produced using snail neurones (Brown, Morimoto, Tsuda & Wilson, 1981; but see Lux & Brown, 1984). Similarly, in cardiac cells, inactivation occurs in conditions that exclude Ca entry (Lee & Tsien, 1982; Reuter, Stevens, Tsien & Yellen, 1982; Cavalié, Ochi, Pelzer & Trautwein, 1983) but it may also show certain characteristics of a Ca current dependence (Kass & Sanguinetti, 1984; Mentrard, Vassort & Fischmeister, 1984; Lee, Marban & Tsien, 1985).

In vertebrate sensory neurones, conditions that isolate Ca currents reveal a transient current around the resting potential (Carbone & Lux, 1984*a*,*b*; Schlichter, Bossu, Feltz, Désarménien & Feltz, 1984; Nowycky, Fox & Tsien, 1984, 1985; Fedulova, Kostyuk & Veselovsky, 1985). This current fits the present electrophysiological definition of a Ca current, although it has distinct characteristics (mainly a reduced inhibitory effect of Cd) when compared to the more classical sustained Ca current (Bossu, Feltz & Thomann, 1985). By its range of activation, this current displays common features with a Ca current encountered in a variety of vertebrate cells (e.g. Hagiwara & Kawa, 1984), in eggs of invertebrates (e.g. Fox, 1981) and in protozoa (Deitmer, 1984). The inactivation process of these various transient Ca currents was concluded to be predominantly under voltage control.

Preliminary observations have revealed that in vertebrate sensory neurones the inactivation curve is shifted along the voltage axis to an extent dependent on the length of the inactivating pulse (Carbone & Lux, 1984*a*; Bossu & Feltz, 1985). Therefore a more detailed investigation of the time course of inactivation was carried out.

The main conclusion of this paper is that inactivation of this Ca current occurs via two kinetic components, a fast component and a slow component. The fast component, from which there is rapid recovery, is only voltage dependent and is responsible for most of the current decline. We present some evidence to show that the slow component has characteristics of a Ca-mediated process, and could delay reinitiation of the transient Ca current ($i_{Ca,t}$).

METHODS

The experiments were carried out on sensory neurones of the IX (petrose) and X (nodose) cranial ganglia. The ganglia excised from new-born rats were treated enzymatically (dispase 5 mg/ml and collagenase 1 mg/ml, for 30 min at 37 °C). After mechanical dissociation, the neurones were plated at 4 ganglia per 35 mm diameter Petri dish coated with rat tail collagen. After short-term culture (3–10 h) in L_{15}-CO_2 (Leibovitz) medium supplemented with 5% rat serum (for details see Bossu *et al.* 1985), neurones reached a stage of development which met the requirements of the patch-clamp technique: (1) they adhered well to the bottom of the culture dish, ensuring mechanical stability; (2) the neurite outgrowth was limited at this stage, giving good voltage-clamp conditions. Enzymes were supplied by Boehringer, Germany, and L_{15}-CO_2 by Gibco, Great Britain.

Recordings were obtained using the whole-cell method of Hamill, Marty, Neher, Sakmann & Sigworth (1981) with an EPC-7 (List Electronic, Germany). Recordings were taken at room temperature (18–22 °C) and stored on a magnetic tape (Racal, Store 4, filter 2·5 kHz). Analysis was performed either by hand on paper traces (Gould, Mark 2200) or on a Plessey 6220 System, DEC compatible. Recordings were displayed without subtraction of leak or capacity currents. Leak current was measured as the current during steps in potential to −100 and −60 mV from a holding potential of −80 mV. Leak current was assumed to be linear in the activation range of threshold Ca current and the extrapolated value was subtracted for quantitative estimates.

Ca currents were recorded in isolation under conditions where Ca was the only permeant cation in the extracellular medium: the external Ca concentration was 5 mM, while the Cs-loaded cytoplasmic side was buffered at pCa 8 using an EGTA (ethylene glycol-bis(β-aminoethyl ether) *N,N'*-tetra-acetic acid)/Ca mixture with a large Ca buffering capacity. The bath solution contained in mM: choline chloride, 130; $CaCl_2$, 5; $MgCl_2$, 2; TEA (tetraethylammonium) Cl, 7·5; HEPES/Tris, 5, at pH 7·4; and glucose, 1 g/l. The pipette solution contained in mM: CsCl, 120; TEA Cl, 20; $MgCl_2$, 2; EGTA/NaOH, 11; $CaCl_2$, 1 (apparent dissociation constant, $K_D = 10^{-7}$ M); HEPES/NaOH, 10, at pH 7·2. The pipette solution was buffered at pCa 7 using a medium of identical composition except with (mM): EGTA/NaOH, 10; $CaCl_2$, 5.

RESULTS

Fig. 1 typifies the main features of the transient Ca current $i_{Ca,t}$ (t for transient) which coexists, in primary sensory neurones, with the more classical sustained Ca current $i_{Ca,s}$ (s for sustained). $i_{Ca,t}$ is a low-threshold current evoked by step depolarizations to beyond −60 mV from a holding potential of −80 mV (Fig. 1*A*). It can be recorded in isolation between −55 mV and about −15 mV, i.e. up to a more or less depolarized membrane potential depending on the amplitude of $i_{Ca,s}$. These two Ca currents usually appear respectively as the minor and major peaks in a current *versus* voltage plot (Fig. 1*B*). For more extensive descriptions of $i_{Ca,t}$, see Carbone & Lux (1984*a*), Bossu *et al.* (1985), Nowycky *et al.* (1984, 1985) and Fedulova *et al.* (1985). The $i_{Ca,t}$ current can readily be identified with the *T* current described by Nowycky *et al.* (1985).

Typically, the rising and decay phases of this inward current were more rapid at more depolarized voltages (Fig. 1*A*). The decay can be approximately fitted by a single exponential: time constants decreased from 126 ms ± 41 at −50 mV ($n = 11$), to 31 ms ± 10 at −20 mV ($n = 11$). In the few cases where $i_{Ca,s}$ had spontaneously vanished, $i_{Ca,t}$ could be recorded up to −10 mV: decay value was then 20 ms ± 7 ($n = 4$). The question arises as to whether the relaxation of this current is due to a developing outward current or to an actual decrease in conductance. In order to measure the underlying conductance tail currents were evoked during the decay phase of $i_{Ca,t}$. Tail currents were measured by repolarizing to −80 mV, where there is a large

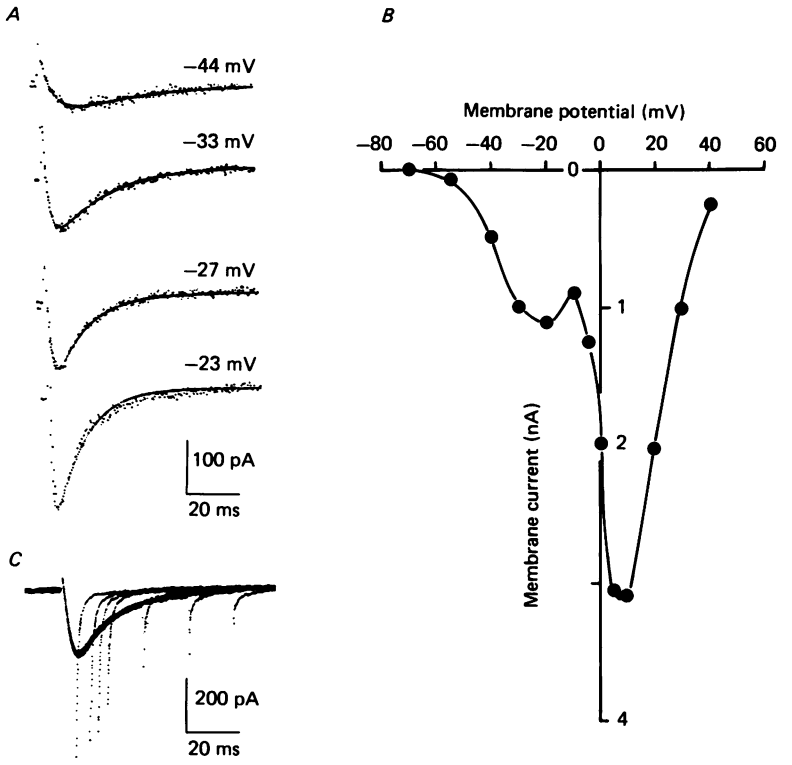

Fig. 1. *A*, single traces of transient Ca current. From a holding potential of −80 mV test pulses to between −55 and −20 mV, elicited a transient inward current (single digitalized traces). The rise and decay phases of the current were fitted by exponentials (corresponding exponential curves have been superimposed). Note that decay could be approximated by a single exponential in all cases except at the most depolarized potential of −23 mV, where a second slow component, which is linked to the development of a sustained Ca current (not shown here) appeared. *B*, a different cell. Current–voltage relation (*I–V* curve) for the peak of the Ca current. At potentials above −10 mV, a sustained Ca current (not studied here) developed and gave rise to the second peak on the *I–V* curve. $i_{Ca,t}$ amplitude was estimated taking the leak current value as a reference when no contaminating $i_{Ca,t}$ was detected. Otherwise the amplitude of $i_{Ca,t}$ was measured from the $i_{Ca,s}$ plateau (namely, the amplitude of the inactivating phase) plus the leak current. $i_{Ca,s}$ was measured at the end of the plateau and the leak current was added. *C*, a different cell. Decay of the transient current corresponds to an actual inactivation. When the potential was stepped back from −20 to −80 mV, the tail current amplitude decreased as the time between peak and return step was increased.

driving force for Ca, after a step to −20 mV which caused channel opening. Tail currents and total current have parallel time courses (Fig. 1*C*), so the decay in Ca current is due to channel inactivation. Outflow through channels not blocked by Cs or TEA can be discounted as such tail currents would increase under these conditions.

Onset of inactivation

The time course of inactivation was examined at different potentials. A similar inactivation could be attained using different pre-pulse potentials if the depolarization was long enough. In Fig. 2*A*, pre-pulses to −37, −40 and −46 mV all led to a 75%

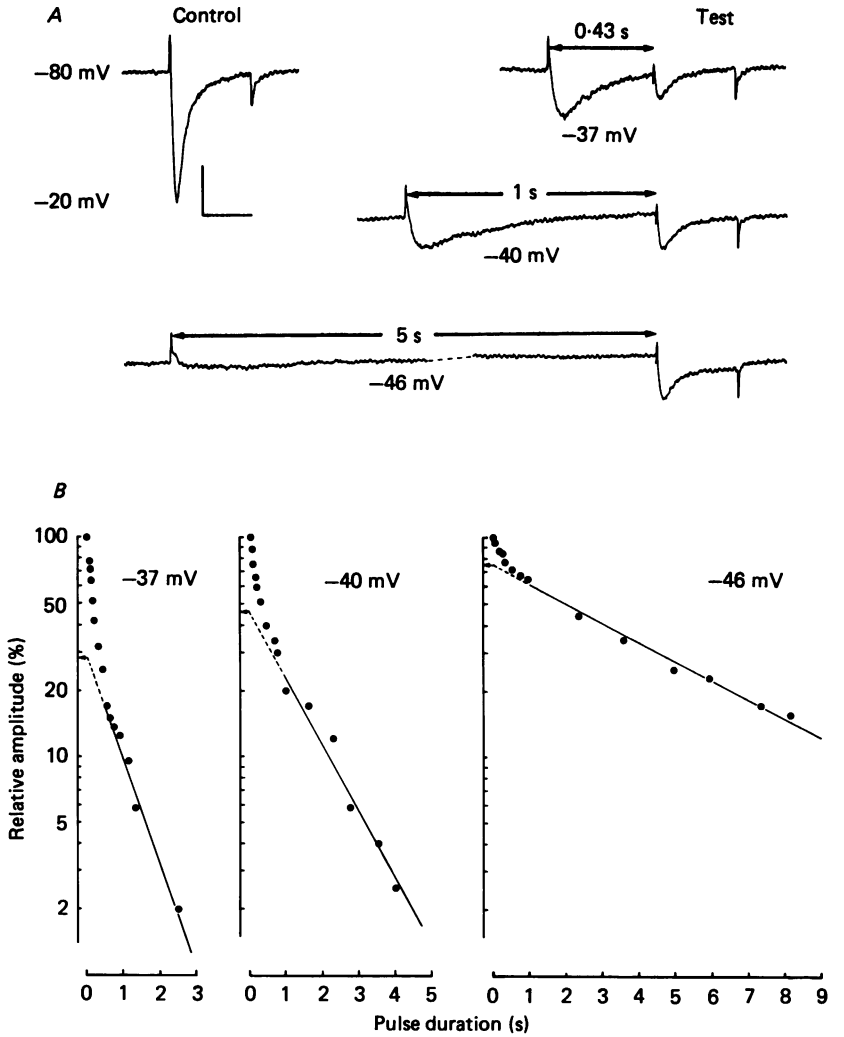

Fig. 2. Time course of inactivation as a function of voltage. *A*, the same relative inactivation of the test response is reached by using longer durations for smaller depolarizing pre-pulses. Pre-pulses were fixed to three distinct values successively and in each case inactivation was followed with time. Single traces shown here correspond to a pre-pulse duration leading to an inactivation of 75%. Control and test responses were elicited by stepping the potential to −20 from −80 mV. Bottom trace is interrupted for 3·2 s (dashed line). Calibration bars: vertical, 100 pA; horizontal, 200 ms. *B*, same cell as in *A*. The semilogarithmic plot of the relative amplitude of the response to test pulse *versus* time is biphasic in all three cases. The exponential fit of the slower component is the only one to be shown (continuous line). The amplitude (arrows) of this component was obtained by back extrapolation to zero time. The respective τ values were 1·2, 1·46 and 4·6 s at −37, −40 and −46 mV. The fast components had correspondingly estimated τ values of 170, 200 and 280 ms.

inactivation of the test response but only after they had been maintained for 0·43, 1 and 5 s respectively. The amplitude of the test response was plotted against the duration of the depolarization pre-pulse. The sum of two exponentials, fast and slow, is needed to describe the data (Fig. 2*B*). The time constants of the fast and slow components of inactivation (τ_f and τ_s respectively) were of the order of a few hundred milliseconds and a few seconds respectively. When the inactivating potential was changed, one phase became dominant: the faster phase at the more depolarized potentials (in Fig. 2*B* on the left, the relative amplitude of the fast component amounts to 72 %), the slower phase at more hyperpolarized levels (in Fig. 2*B* on the right, the relative amplitude of the slow component reaches 78 %). In extreme cases, one or the other phase could be absent entirely. These data suggest that a slow inactivation process prevails at more hyperpolarized potentials whereas for larger depolarizations the transition towards the inactivated state mainly occurs through a fast process.

Both τ_f and τ_s tended to be smaller for the more depolarizing pre-pulses. However, only a narrow range of potentials could be investigated in each case (about 10 mV). In the experiment illustrated in Fig. 2, τ_f values decreased from 280 to 120 ms, and τ_s values from 4·6 to 1·2 s when inactivating pulses were varied from −46 mV to −37 mV. At −20 mV, the single measurable τ was 50 ms. We have calculated, assuming a constant voltage dependence of the time constants, that at −55 mV τ_f and τ_s would be 500 ms and 5 s respectively. Furthermore, at a given pre-pulse depolarization values varied greatly. For three cells at −45 mV τ_f was between 100 and 280 ms and τ_s was between 1 and 4·6 s; at −20 mV τ_f varied between 10 and 50 ms whereas τ_s was absent. So the value of τ_f at depolarized potentials is in the same range as the time constant of the decay.

Recovery from inactivation

The time course of recovery depended on the duration of the inactivating pulse. Two protocols were used: the inactivating voltage was either applied as a 300 ms duration pulse from a holding potential of −80 mV (Fig. 3) or maintained (Fig. 4). After an inactivating period, the amplitude of the response to the test pulse was clearly a function of the duration of the recovery at −80 mV. The response after 1 min recovery was defined as the control.

After a short inactivating pre-pulse (300 ms), the rate of recovery varied greatly (compare cells *a* and *c* in Fig. 3*A*). Interestingly, recovery from inactivation occurred according to one (cell *a*) or two (cells *b* and *c*) exponentials. The faster component had an average time constant of 253 ms ± 59 ($n = 20$, S.D.) and 81 % ± 19 of the recovery was through this process. Full recovery extended over a few seconds: the slow component had a time constant of 1·52 s ± 0·45 ($n = 10$, S.D.) but only accounted for 34 % ± 14 ($n = 10$, S.D.) of the recovery process, and in ten other cases it was not detectable. Conversely, after long inactivating pre-pulses recovery was mostly a slow process (Fig. 4): the slow component had a time constant of 4·0 s ± 1·1 ($n = 6$, S.D.) and represented 83 % ± 13 of recovery. In some cases (four out of six), recovery nevertheless started with a small (25 % ± 6; $n = 4$, S.D.) fast component of 510 ms ± 95 ($n = 4$, S.D.). When one compares recovery after short and long inactivating pulses both τ values are greater by a factor of two to three after maintained depolarization.

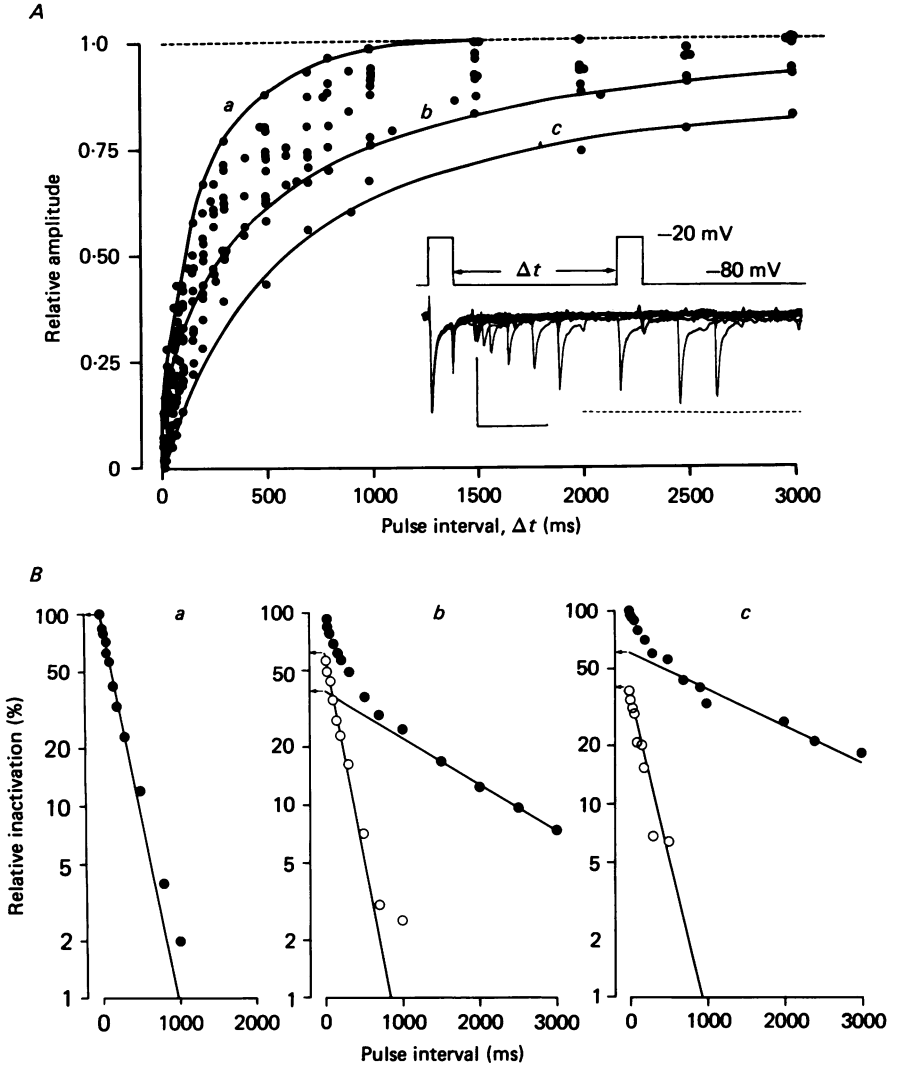

Fig. 3. Time course of recovery after short-term inactivation. *A*, a 300 ms test pulse to −20 mV from a holding potential of −80 mV evoked a response which was inactivated by a preceding pulse of the same amplitude and duration. The inset shows superimposed traces from successive trials in a single experiment where the pulse interval was progressively increased (dashed line shows the amplitude of the control response). Calibration bars: vertical, 100 pA; horizontal, 1 s. Relative amplitude of response to test pulse compared to control response was plotted against pulse interval. Data, shown in *A*, were gathered over eleven similar experiments. Continuous curves (*a*, *b*, *c*) are based on data from three different cases. *B*, for above cells *a*, *b* and *c*, the percentage relative inactivation was estimated by the ratio $((1-i_c/i_t)\%)$, where i_c and i_t refer to the amplitude of the responses to the control and test pulses respectively. This ratio has been plotted in *a*, *b* and *c* respectively as a function of the pulse interval (semilogarithmic plot). A single exponential was used to describe *a*, and double exponentials to describe *b* and *c*. In this Figure, as in the three subsequent ones, the filled circles give the over-all current and open circles give the current remaining after subtraction of the slow component. A similar fast component, with τ values of 200, 210 and 230 ms was found in *a*, *b* and *c* respectively. The slow component in *b* and *c* had a time constant of 1·7 and 2·3 s respectively. The arrows point to the amplitude of each component measured by back extrapolation to zero time.

Thus in both the inactivation process and in the recovery from inactivation there were two distinct kinetic components, one fast, the other slow. Moreover, when the fast process of inactivation was favoured, recovery proceeded via the faster component; the inverse was also true, i.e. slow inactivation, slow recovery. This led us to propose that the two inactivation processes represent two distinct inactivated states: I_f (fast)

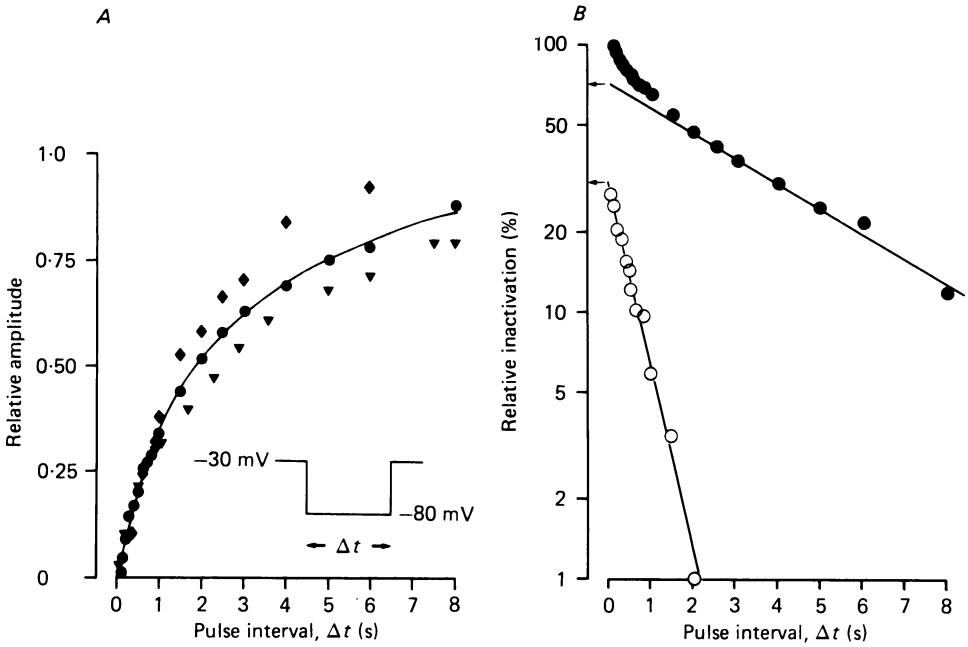

Fig. 4. Time course of recovery after long-term inactivation. *A*, a hyperpolarizing pulse to −80 mV ended inactivation resulting from maintained depolarization (>20 s) to −30 mV: a transient inward current developed when potential was stepped back to −30 mV (see also Fig. 7*A*). Its amplitude i_t, was compared to the amplitude of the control response, i_c (obtained by a step to −30 mV from a potential of −80 mV maintained for at least 20 s) and plotted against the duration Δt of the hyperpolarizing pulse (three different cells). *B*, semilogarithmic plot of the relative percentage inactivation ($[1-i_t/i_c]\%$) against Δt (for the cell represented in *A* by the filled circle and with curve fitted by eye) illustrates the biphasic recovery. The time constants were 0·65 s and 4·2 s for the fast and slow components respectively.

and I_s (slow). To illustrate this hypothesis we monitored recovery from both processes in the same cell. In the case shown in Fig. 5, after a 300 ms pulse, the slow component of recovery was already quite large (as was the case for cell *c* in Fig. 3), but it became prominent, accounting for 86% of recovery, after a 1 s inactivating pulse, which favoured the slow onset of inactivation. It is also possible to bring out fast or slow inactivation and recovery processes by modifying the potential of the inactivating pre-pulse. The relative amplitude of recovery by the fast mechanism increased from 34% ± 8 for a pre-pulse to −40 mV up to 92% ± 11 for a pre-pulse to −20 mV in seven cells. To test which phase was effectively modified we compared the absolute values of the current carried. The amplitude of the slow component of recovery was the same, regardless of whether the 300 ms inactivating pulses were given to −20 mV or to

−40 mV; the amplitude of the fast component increased with increased potential (Fig. 6). This does not mean that there is no voltage effect on the slow component; the slow rate of recovery was on average faster for a conditioning pulse to −40 mV (0·85 s±0·15; $n = 6$, S.D.) than for one to −20 mV (about 1·5 s) whereas τ_f was the same: 232 ms±79 ($n = 4$, S.D., compared to about 250 ms at −20 mV). This is somewhat in contrast to what we observed at the onset of inactivation, since in this case more depolarized inactivating pre-pulses accelerated both time constants.

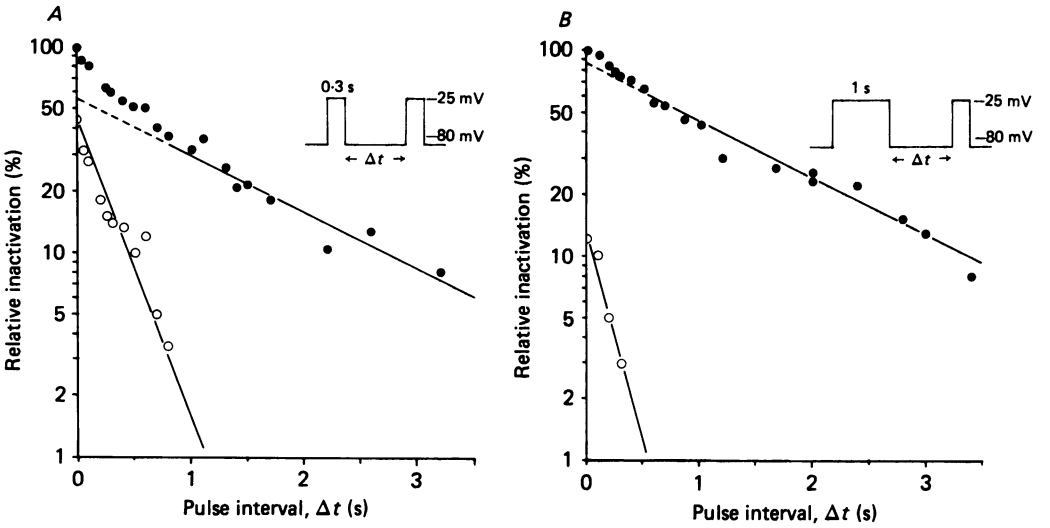

Fig. 5. Recovery of inactivation as a function of the duration of the inactivating pulse. The inactivating pulse was a depolarization to −25 mV from a holding potential of −80 mV; in *A* the inactivating pulse was short (300 ms); in *B* it was long (1 s). A single cell. *A* and *B*, semilogarithmic plots of the amplitude of the test response as compared to the amplitude of the control response *versus* the recovery pulse interval, Δt. A dual exponential fit was used. The slower component had a time constant of 1·54 and 1·51 s in *A* and *B* respectively; fast recovery showed time constants of 310 and 170 ms, respectively.

We observed another voltage effect that was dependent on the potential of the reactivating pulse. As shown in Fig. 7, inactivation at pCa 8 resulting from a prolonged depolarization could be relieved by a hyperpolarizing step to −80 mV or to −100 mV, two potentials which *per se* do not induce any inactivation. Recovery, although slow as expected, was faster when the hyperpolarizing potential was −100 mV than when it was −80 mV. Conversely, the onset of the slow component was found to be accelerated when the membrane potential was more depolarized (cf. Fig. 2*B*). Two phases were therefore revealed both at the onset and at the offset of the inactivation, and we could already conclude that the two processes involved were not interdependent.

Voltage dependence of the two components of inactivation

The inactivation which leads to channel closing was characterized using the classical double-pulse protocol. The amplitude of the current elicited by a test pulse

of fixed amplitude was measured when the amplitude of a conditioning pulse was varied. We routinely used 300 ms and 10 s pre-pulses to investigate the fast and slow components of inactivation respectively.

A typical experiment is illustrated in Fig. 8, where the duration of the pre-pulse was 300 ms and the test pulse brought the membrane potential to −20 mV. Fig. 8*A* (right column) shows the traces obtained, and the characteristics of the inactivation

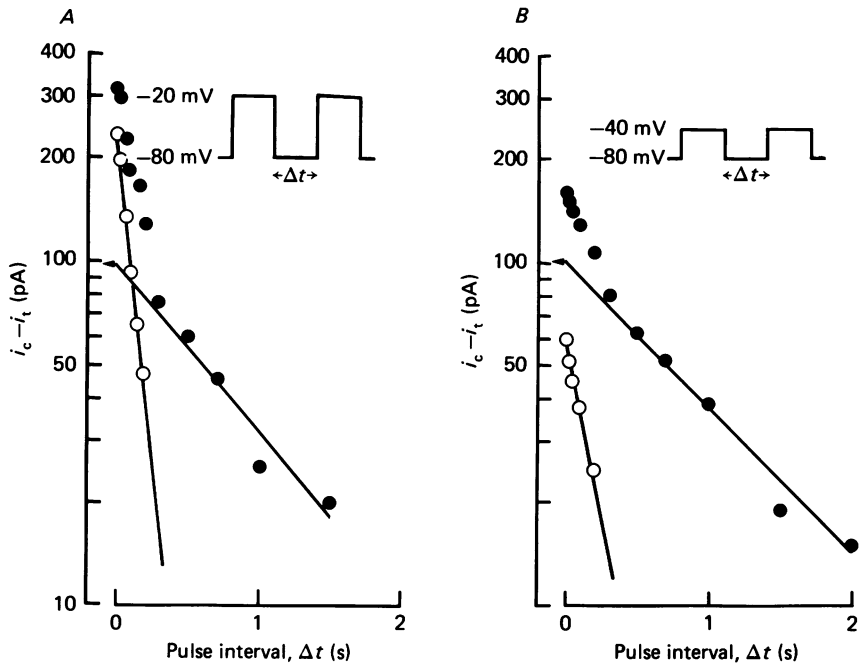

Fig. 6. The time course of recovery as a function of the potential of the inactivating pulse. Inactivation was initiated by a short pre-pulse of 300 ms from a holding potential of −80 mV to either −20 mV (*A*) or −40 mV (*B*). A single cell. The difference between the amplitudes (in pA) of the control current i_c and the test current i_t inactivated by the depolarizing prepulse is plotted *versus* the pulse interval (semilogarithmic plot). The time course was approximated by two exponentials. The slow components, of identical amplitude (arrows), had time constants of 0·90 and 1·05 s in *A* and *B* respectively; note that on average, this τ value was smaller at more depolarized potentials. The τ values of the fast components were 120 and 200 ms respectively.

processes are illustrated in Fig. 8*B* (filled circles). This inactivation curve has a negative slope between −60 and −20 mV, the precise voltage range over which the conditioning pulse evoked a response. Typically, all inactivation curves displayed a steep voltage dependence, with a slope with a k value of $-4{\cdot}2 \pm 1{\cdot}1$ ($n = 9$) in an S-shape fit where a formulation of the type $i = 1/(1+\exp(V'-V)/k)$ was used, where V' is the potential for half maximum conductance and k is a slope constant. In the other cases (nine out of a sample of eighteen), above −50 mV the voltage dependence was obviously less steep but no explanation for this was found. For test pulses to −20 mV, 50 % inactivation was attained at $-47{\cdot}7$ mV $\pm 4{\cdot}1$ ($n = 18$, S.D.), and the linear part of the curve corresponded to an inactivation of $5{\cdot}7\,\% + 1{\cdot}3$ ($n = 18$, S.D.) per mV.

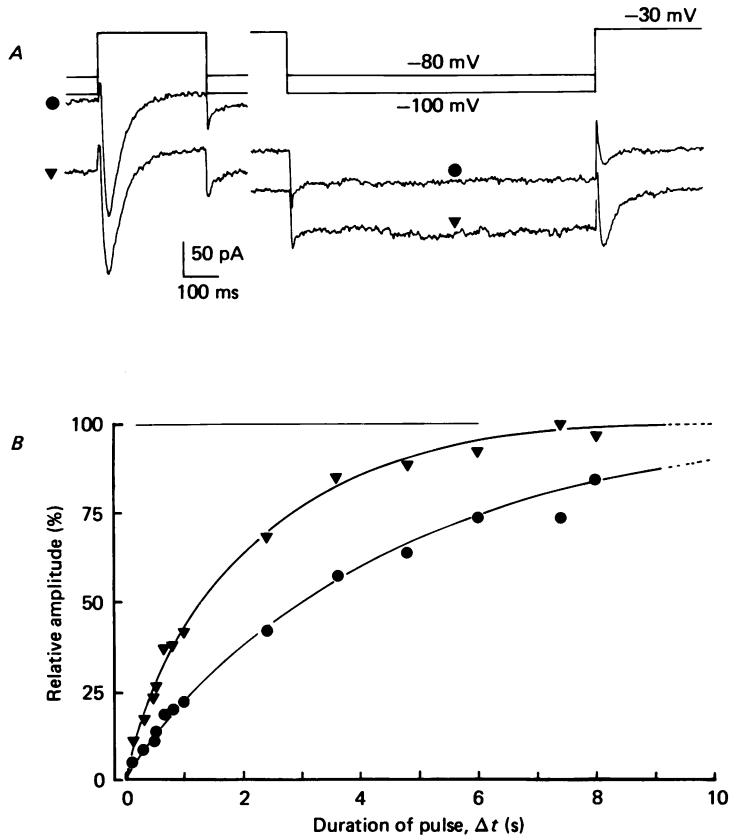

Fig. 7. Recovery from slow inactivation depends on the value of the repolarizing potential. At pCa 8, same protocol as in Fig. 4. *A*, traces on the left show control responses obtained by stepping the potential to −30 mV from a holding potential of −100 mV (▼) or −80 mV (●). Traces on the right, inactivation induced by holding the potential at −30 mV was partially relieved by an 850 ms hyperpolarizing pulse to either −100 mV (▼) or −80 mV (●). Note that traces have been shifted for clarity. *B*, recovery of inactivation was followed *versus* the duration of the hyperpolarizing pulse. Recovery was characterized by a slow component which was faster when the hyperpolarizing potential was −100 mV (▼, $\tau = 3{\cdot}1$ s) than when it was −80 mV (●, $\tau = 4{\cdot}4$ s).

Slow inactivation characteristics were obtained with the longer pre-pulse and the application of a single test pulse (Fig. 8*A*, left column). The main effect was to shift the inactivation curve towards more hyperpolarized potentials (Fig. 8*B*, filled diamonds). Inactivation to 50% was attained at -64 mV± 3 ($n = 5$, S.D.) and inactivation over the linear part of the curve corresponded to a reduction of $4{\cdot}7\% \pm 1{\cdot}4$ per mV.

For test pulses to −30 mV, the mid-point of the inactivation curves was attained at -58 mV± 2 ($n = 5$, S.D.) and -65 mV± 3 when using the short and long inactivating pulses respectively.

Ca ions and the inactivation processes

Ca entry. Because of the variability in the relative contribution of I_f and I_s to inactivation, we investigated a possible Ca effect through Ca entry. We excluded this possibility for the fast inactivation which displays the characteristics of a purely voltage-dependent process. (1) Manipulation of Ca ions did not alter the decay of the current taken as an index of the I_f process. Namely, no change was observed when

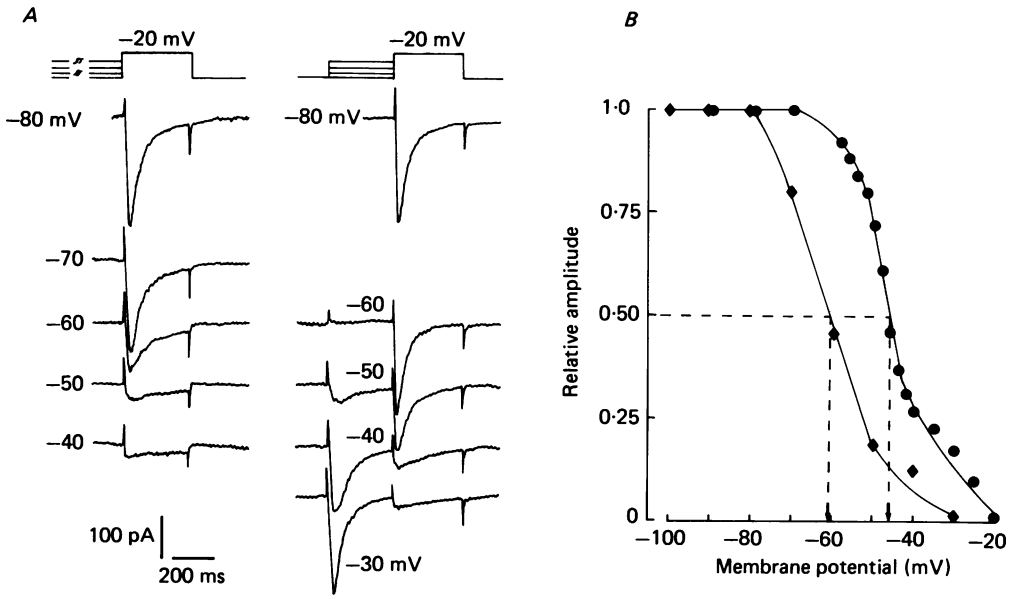

Fig. 8. Slow and fast inactivation as a function of potential. *A*, the amplitude of the response to a step potential to −20 mV from a holding potential of −80 mV (top traces) was reduced by a preceding depolarization. When the pre-pulse was of long duration (10 s, shown interrupted by // in the Figure) the I_s component was preponderant (left column), whereas the I_f component was preponderant after a pre-pulse of short duration (300 ms, right column). The value of the pre-pulse potential is given for each trace. *B*, the non-inactivated fraction of the transient Ca current during the test pulse is plotted against the conditioning voltage, same cell as in *A*. Inactivation by 50 % was induced by a pre-pulse to −46 and −61 mV of duration 300 ms (●) or 10 s (◆) respectively. The slope of the voltage effect, characterized by a linear fit, is 4 % per mV and 3 % per mV respectively.

the external Ca concentration was changed or when Ba was substituted for Ca. In the same cell the time constants of decay in 2 mM-Ca, 10 mM-Ca and 10 mM-Ba were 41, 39 and 44 ms at −40 mV; 30, 28 and 32 ms at −30 mV respectively. Comparing different cells, the time constants of decay in ms were 30 ± 5 ($n = 3$) and 48 ± 23 ($n = 3$) in 5 mM-Ba and 42 ± 14 ($n = 15$), 78 ± 30 ($n = 14$) in 5 mM-Ca at −20 and −30 mV respectively. (2) Further, as shown in Fig. 9*A* decay did not depend on the quantity of current flowing but on the membrane potential. (3) Finally, inactivation did not recede at those potentials where Ca entry was reduced as a result of a reduced driving force on the Ca ions. As Fig. 9*B* (open circles) illustrates, there was a monotonic

decrease of the response for the fast inactivation process, this being investigated with very short time lags (here 30 ms) between the inactivating and the test pulses.

In contrast, slow inactivation displayed some features of Ca dependence. (1) The classical double pulse protocol was adapted so as to compare fast and slow inactivation on a single cell. If a 300 ms recovery period is used instead of the 30 ms

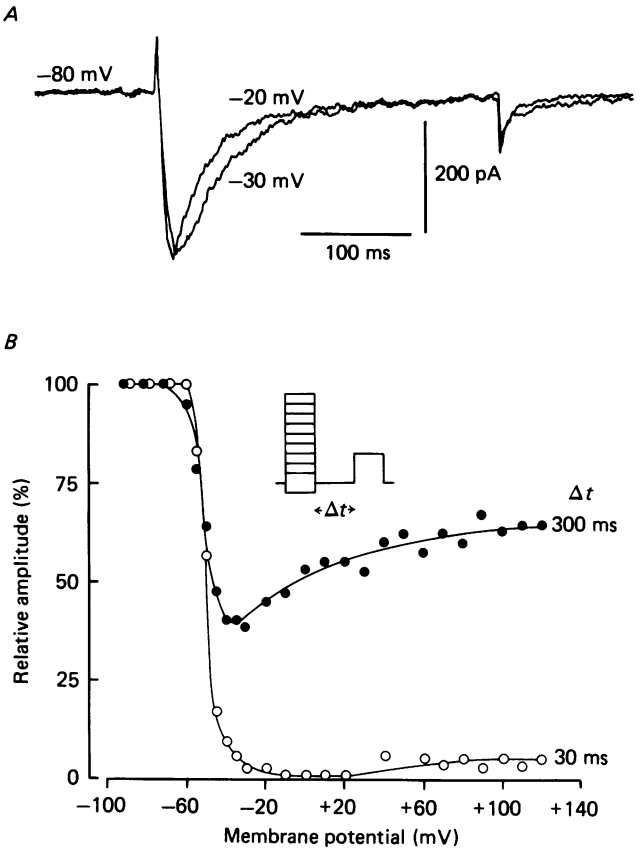

Fig. 9. *A*, single traces obtained when the membrane potential was brought successively to −30 and −20 mV from a holding potential of −80 mV. Note that the decay rates differed although the initial Ca entry was the same. *B*, the shape of the inactivation curve depends on the duration of the time interval, Δt, between the inactivating and the test pulses. Same protocol as in Fig. 4, but the potential of the inactivating pulse was varied from −100 up to +140 mV. The pulse interval, Δt, was either 30 (○) or 300 ms (●). A single cell where $i_{Ca,t}$ reached a peak value at −25 mV and $i_{Ca,s}$ reached a peak value at 0 mV.

period used to characterize I_f, fast recovery should be over and the process under study will be slow inactivation. Fig. 9*B* (filled circles) illustrates one of the cases where the inactivation curve was somewhat U-shaped after a 300 ms recovery period. The flattening of the U-curve could be a result of the protocol we used: a fast inactivation could still be present after 300 ms. The alternative hypothesis is that it is due to specific I_s characteristics, on which a combination of voltage- and Ca-dependent

mechanisms is acting. In Fig. 9 such mechanisms would then amount respectively to a 40% inactivation and an additional 20% inactivation at maximal Ca entry around −20 mV. If Ca is involved here (see discussion in Lee *et al.* 1985), it could be entering the cell through the $i_{Ca,t}$ channels as the U-shaped voltage dependence of inactivation mirrors the current–voltage curve for $i_{Ca,t}$ (Fig. 1 this paper, and Fig. 3*A* in Bossu *et al.* 1985). (2) A long inactivating pulse induced a current deficit in a test response without a steady state being attained. In fact a second test pulse induced a further reduction in the response when it was compared to the first test response. This effect was independent of the duration of the long inactivating pulse (10 s or 30 s), but depended on the time interval between each test pulse. The response decrease following a test pulse could originate from entry of Ca since this decrease was larger after responses of larger amplitude.

Internal Ca concentration. These observations prompted us to investigate the effect of changes of the internal Ca concentration. When the cytoplasm was dialysed with a pipette solution at pCa 7, equilibration was monitored by holding the potential at −80 mV and following the response to test pulses to −30 mV. At pCa 7, responses typically decreased before reaching a steady amplitude within 5 min and at this stage maximal response was obtained by hyperpolarizing the cell to −100 mV. Therefore for all experiments, whatever the pCa to be studied, the equilibration time was fixed at 5 min. The holding potential was chosen at −100 mV to allow maximal response in all cases and test pulses depolarized the cell to −30 mV so as to minimize contamination by the 'high-threshold' currents. The current–voltage curve and the two types of inactivation curves were then established. A comparison of the data obtained at Ca concentrations of 5×10^{-10} and 10^{-7} M showed that the current threshold was shifted towards more hyperpolarized potentials at the higher internal Ca concentration: between 5 and 10 mV, with almost no change in the voltage-eliciting peak values (still around −30 mV). The two inactivation curves were also shifted towards more hyperpolarized potentials when the internal Ca concentration was increased but in distinct domains of internal pCa. When short inactivating pulses were used, a slight displacement of the inactivation curve occurred when the Ca concentration was varied from 5×10^{-10} to 10^{-8} M: mid-points were at $-52 \text{ mV} \pm 1$ ($n = 4$) and $-58 \text{ mV} \pm 2$ ($n = 5$) respectively. At pCa 7, the mid-point value was almost identical to that observed at pCa 8 ($-60 \text{ mV} \pm 3$, $n = 5$). In contrast, when long inactivating pulses were used a clear shift of the curves occurred when the internal Ca concentration was varied from 10^{-8} to 10^{-7} M: the mid-points were at $-65 \text{ mV} \pm 3$ ($n = 5$) and $-74 \text{ mV} \pm 3$ ($n = 5$) respectively, whereas the inactivation curves at 5×10^{-10} and 10^{-8} M-Ca were superposed (mid-point at $-65 \text{ mV} \pm 1$, $n = 4$ in the former case).

DISCUSSION

In the present work, we show that inactivation of the transient low-threshold Ca current in rat sensory neurones proceeds along two phases which are probably not interdependent. A biphasic inactivation was also observed by Brown *et al.* (1981) when studying the high-threshold Ca current in snail neurones where a slow inactivation accounts for most of the current decline. Here, fast inactivation is mainly

seen during the decay of $i_{Ca,t}$ and slow inactivation is likely to be the major element controlling its repriming.

The idea that Ca entry and its accumulation are required for inactivation was first suggested by Brehm & Eckert (1978) and Tillotson (1979). The main evidence being (1) the decay of the current was accelerated by increasing the external Ca concentration and when Ca was substituted for Ba; (2) the decay was further modified by Ca or EGTA injection (i.e. changing the internal Ca concentration); and (3) the U-shape of the inactivation curve when the amplitude of the depolarizing pre-pulses was increased: first entry increased and then it decreased as a result of a reduced driving force on the Ca ions (see Eckert & Chad, 1984, for a review). For the fast inactivation, and the decay of $i_{Ca,t}$ taken as its index, none of these criteria were fulfilled: we therefore conclude that fast inactivation is only voltage dependent. Similarly, current decline was observed on averaged traces of single channel recordings, a condition where no ionic accumulation takes place whether Ba or Ca is the permeant cation (Carbone & Lux, 1984*b*; Nowycky *et al.* 1985). This inactivation is reminiscent of the process terminating Ca current in polychaete egg cells (Fox, 1981). In contrast, Ca entry has some effect on the inactivation subsequent to a long depolarization. It is best evidenced as a further 'use-dependent' decrease of the response on the application of successive test pulses after a holding potential inducing slow inactivation. This control would operate on an inactivating gate. So, Ca intervenes in the inactivation of both $i_{Ca,t}$ and $i_{Ca,s}$. At internal Ca concentrations above 10^{-7} M, $i_{Ca,t}$ is recorded in isolation; its inactivating site therefore has a rather low affinity for internal Ca. In vertebrate cells, Kostyuk (1984) estimated the K_D for $i_{Ca,s}$ inactivation to be around 10^{-8} M, at least one order of magnitude less.

In addition, internal Ca alters the voltage-sensitivity of the $i_{Ca,t}$ channel in all its configurations, activated or inactivated. Investigations should be performed varying the Ca concentration from 10^{-9} to 10^{-6} M, which is the probable range over which Ca concentrations fluctuate in connexion with metabolism or in response to external signals. But the present results, obtained at 10^{-7} M, suggest that Ca permeation, like K permeation (see Marty 1983, for a review), is under the double control of membrane potential and the internal bulk Ca concentration. Ca permeability is sensitive to voltage around the resting potential, whereas K permeability is modified by more depolarized potentials. Defining the characteristics of the controls exerted on $i_{Ca,t}$ may reveal a widespread mechanism for the control of Ca entry.

We thank Dr B. Demeneix and Dr J.-L. Rodeau for their helpful comments and careful reading of the manuscript. We are grateful to Mrs E. Mioskowski for technical assistance and to Mr S. Liess for help in the preparation of this manuscript. We acknowledge financial support from CNRS and the Université Louis Pasteur, Strasbourg, and thank CNRS (ATP 5283) and INSERM (CRE 84 6009) for the award of grants to A. F.

REFERENCES

ASHCROFT, F. M. & STANFIELD, P. R. (1981). Calcium dependence of the inactivation of calcium currents in skeletal muscle fibers of an insect. *Science* **213**, 224–226.

BOSSU, J.-L. & FELTZ, A. (1985). Inactivation of the low threshold Ca current elicited in vertebrate sensory neurones is a biphasic process. *Neuroscience Letters*, suppl, **22**, S417.

BOSSU, J.-L., FELTZ, A. & THOMANN, J. M. (1985). Depolarization elicits two distinct calcium currents. *Pflügers Archiv* **403**, 360–368.

BREHM, P. & ECKERT, R. (1978). Calcium entry leads to inactivation of calcium in *Paramecium*. *Science* **202**, 1203–1206.

BROWN, A. M., MORIMOTO, K., TSUDA, Y. & WILSON, D. L. (1981). Calcium current-dependent and voltage-dependent inactivation of calcium channels in *Helix aspersa*. *Journal of Physiology* **320**, 193–218.

CARBONE, E. & LUX, H. D. (1984*a*). A low voltage-activated calcium conductance in embryonic chick sensory neurons. *Biophysical Journal* **46**, 413–418.

CARBONE, E. & LUX, H. D. (1984*b*). A low voltage-activated, fully inactivating Ca channel in vertebrate sensory neurones. *Nature* **310**, 501–502.

CAVALIÉ, A., OCHI, R., PELZER, D. & TRAUTWEIN, W. (1983). Elementary currents through Ca channels in guinea pig myocytes. *Pflügers Archiv* **398**, 284–297.

DEITMER, J. W. (1984). Evidence for two voltage-dependent calcium currents in the membrane of the ciliate *Stylonychia*. *Journal of Physiology* **355**, 137–159.

ECKERT, R. & CHAD, J. E. (1984). Inactivation of Ca channels. *Progress in Biophysics and Molecular Biology* **44**, 215–267.

ECKERT, R., TILLOTSON, D. L. & BREHM, P. (1981). Calcium-mediated control of Ca and K currents. *Federation Proceedings* **40**, 2226–2232.

FEDULOVA, S. A., KOSTYUK, P. G. & VESELOVKSY, N. S. (1985). Two types of calcium channels in the somatic membrane of new-born rat dorsal root ganglion neurones. *Journal of Physiology* **359**, 431–446.

FOX, A. P. (1981). Voltage-dependent inactivation of a calcium channel. *Proceedings of the National Academy of Sciences of the U.S.A.* **78**, 953–956.

HAGIWARA, S. & BYERLY, L. (1981). Calcium channel. *Annual Review of Neuroscience* **4**, 69–125.

HAGIWARA, S. & KAWA, K. (1984). Calcium and potassium currents in spermatogenic cells dissociated from rat seminiferous tubules. *Journal of Physiology* **356**, 135–149.

HAGIWARA, S. & NAKAJIMA, S. (1966). Effects of the intracellular Ca ion concentration upon the excitability of the muscle fiber membrane of a barnacle. *Journal of General Physiology* **49**, 807–818.

HAMILL, O. P., MARTY, A., NEHER, E., SAKMANN, B. & SIGWORTH, F. J. (1981). Improved patch clamp techniques for high resolution current recording from cells and cell-free membrane patches. *Pflügers Archiv* **391**, 85–100.

KASS, R. S. & SANGUINETTI, M. C. (1984). Inactivation of calcium channel current in the calf cardiac Purkinje fiber. Evidence for voltage- and calcium-mediated mechanisms. *Journal of General Physiology* **84**, 705–726.

KOSTYUK, P. G. (1984). Intracellular perfusion of nerve cells and its effects on membrane currents. *Physiological Reviews* **64**, 435–454.

KOSTYUK, P. G. & KRISHTAL, O. A. (1977). Effects of calcium and calcium-chelating agents on the inward and outward current in the membrane of mollusc neurones. *Journal of Physiology* **270**, 569–580.

LEE, K. S., MARBAN, E. & TSIEN, R. W. (1985). Inactivation of calcium channels in mammalian heart cells: joint dependence on membrane potential and intracellular calcium. *Journal of Physiology* **364**, 395–411.

LEE, K. S. & TSIEN, R. W. (1982). Reversal of current through calcium channels in dialysed single heart cells. *Nature* **297**, 498–501.

LUX, H. D. & BROWN, A. M. (1984). Single channel studies on inactivation of calcium currents. *Science* **225**, 432–434.

MARTY, A. (1983). Ca-dependent K channels with large unitary conductance. *Trends in Neuroscience* **6**, 262–265.

MENTRARD, D., VASSORT, G. & FISCHMEISTER, R. (1984). Calcium-mediated inactivation of the calcium conductance in caesium-loaded frog heart cells. *Journal of General Physiology* **83**, 105–131.

NOWYCKY, M. C., FOX, A. & TSIEN, R. W. (1984). Two types of Ca channel in cultured DRG cells. In *Electropharmacology of the In Vitro Synapse*. Satellite symposium of the 9th International Pharmacological Congress at St. Andrews.

NOWYCKY, M. C., FOX, A. P. & TSIEN, R. W. (1985). Three types of neuronal calcium channel with different calcium agonist sensitivity. *Nature* **316**, 440–443.

PLANT, T. D., STANDEN, N. B. & WARD, T. A. (1983). The effects of injection of calcium ions and calcium chelators on calcium channel inactivation in *Helix* neurones. *Journal of Physiology* **334**, 189–212.

REUTER, H., STEVENS, C. F., TSIEN, R. W. & YELLEN, G. (1982). Properties of single calcium channels in cardiac cell culture. *Nature* **297**, 501–504.

SCHLICHTER, R., BOSSU, J.-L., FELTZ, A., DÉSARMÉNIEN, M. & FELTZ, P. (1984). Characterization of the multiple currents underlying spike activity in sensory neurones: An attempt to determine the physiological role of GABA-B receptor activation on slow conducting primary afferents. *Neuropharmacology* **23**, 869–872.

TAKAHASHI, K. & YOSHII, M. (1978). Effects of internal free calcium upon the sodium and calcium channels in the tunicate egg analysed by the internal perfusion technique. *Journal of Physiology* **279**, 519–549.

TILLOTSON, D. (1979). Inactivation of Ca conductance dependent on entry of Ca ions in Molluscan neurons. *Proceedings of the National Academy of Sciences of the U.S.A.* **76**, 1497–1500.

TSIEN, R. W. (1983). Calcium channels in excitable cell membranes. *Annual Review of Physiology* **45**, 341–358.